The Journal of Experimental Biology 203, 2737–2745 (2000)
Printed in Great Britain © The Company of Biologists Limited 2000
JEB2914

IN VIVO DEMONSTRATION OF LOAD-INDUCED FLUID FLOW IN THE RAT TIBIA AND ITS POTENTIAL IMPLICATIONS FOR PROCESSES ASSOCIATED WITH FUNCTIONAL ADAPTATION

M. L. KNOTHE TATE[1,2,*], R. STECK[1,2], M. R. FORWOOD[3] AND P. NIEDERER[1]

[1]*Institute of Biomedical Engineering and Medical Informatics, University and Swiss Federal Institute of Technology, Gloriastrasse 35/ETZ, CH-8092 Zurich, Switzerland,* [2]*AO/ASIF Research Institute, Davos, Switzerland* and [3]*Department of Anatomical Sciences, University of Queensland, Brisbane, Australia*

*e-mail: tate@biomed.ee.ethz.ch

Accepted 23 June; published on WWW 22 August 2000

Summary

Load-induced extravascular fluid flow has been postulated to play a role in mechanotransduction of physiological loads at the cellular level. Furthermore, the displaced fluid serves as a carrier for metabolites, nutrients, mineral precursors and osteotropic agents important for cellular activity. We hypothesise that load-induced fluid flow enhances the transport of these key substances, thus helping to regulate cellular activity associated with processes of functional adaptation and remodelling. To test this hypothesis, molecular tracer methods developed previously by our group were applied *in vivo* to observe and quantify the effects of load-induced fluid flow under four-point-bending loads. Preterminal tracer transport studies were carried out on 24 skeletally mature Sprague Dawley rats. Mechanical loading enhanced the transport of both small- and larger-molecular-mass tracers within the bony tissue of the tibial mid-diaphysis. Mechanical loading showed a highly significant effect on the number of periosteocytic spaces exhibiting tracer within the cross section of each bone. For all loading rates studied, the concentration of Procion Red tracer was consistently higher in the tibia subjected to pure bending loads than in the unloaded, contralateral tibia. Furthermore, the enhancement of transport was highly site-specific. In bones subjected to pure bending loads, a greater number of periosteocytic spaces exhibited the presence of tracer in the tension band of the cross section than in the compression band; this may reflect the higher strains induced in the tension band compared with the compression band within the mid-diaphysis of the rat tibia. Regardless of loading mode, the mean difference between the loaded side and the unloaded contralateral control side decreased with increasing loading frequency. Whether this reflects the length of exposure to the tracer or specific frequency effects cannot be determined by this set of experiments. These *in vivo* experimental results corroborate those of previous *ex vivo* and *in vitro* studies. Strain-related differences in tracer distribution provide support for the hypothesis that load-induced fluid flow plays a regulatory role in processes associated with functional adaptation.

Key words: load-induced fluid flow, *in vivo* study, functional adaptation, mechanotransduction, molecular transport, tracer, bone, rat, tibia.

Introduction

Although sometimes initiated by short-term events, processes associated with functional adaptation typically require months or years for consummation. This adaptive response to changes in mechanical stimuli has been documented from an *a priori* perspective in a variety of *in vivo* animal models including the functionally isolated avian ulna model of Rubin and Lanyon (1984), the four-point-bending model of the rat tibia of Turner et al. (1991), the rat tail vertebrae loading model of Chambers et al. (1993) and the rat ulna model of Torrance et al. (1994).

Recently, cell biologists have used these *in vivo* and other *in vitro* models to examine cell activity in response to short-term changes in mechanical loading. A single, short period of mechanical loading has been shown to increase the uptake of [^{3}H]uridine by osteocytes in the cortex of the functionally isolated avian ulna (Pead et al., 1988). Short periods of hyperphysiological mechanical loading have been shown to increase bone formation and to decrease resorptive activity in the rat ulna (Hillam and Skerry, 1995). Although osteocytes have been shown to express mRNA for β-actin, osteocalcin, connexin-43, iGF-I, c-*fos* and c-*jun in vivo*, short-term loading of the rat ulna has not been shown to alter the expression of these genes *in vivo* (Mason et al., 1996). In addition, osteocytes appear to show a response to shear stresses similar to that of endothelial cells and neurons, which respond by releasing prostaglandins and/or nitric oxide metabolites. Both these

products help to regulate signal transmission throughout the cellular network (Frangos et al., 1985; Dawson and Snyder, 1994; Pitsillides et al., 1995; Klein-Nulend et al., 1995; Fox et al., 1995; Turner et al., 1995). Finally, a potential role of ion channels within cell membranes in mediating cellular response to changes in mechanical loading has been postulated (Cowin et al., 1991), and *in vitro* studies have demonstrated the involvement of a variety of ion channels in the early response of osteoblasts and osteocytes to mechanical strain (Rawlinson et al., 1996).

Despite the obvious contribution of these studies to an understanding of cellular activity associated with the processes of modelling and remodelling, the actual mechanisms by which cells perceive and respond to changes in their mechanical environment remain unclear. Recently, attention has shifted from mechanisms involving mechanical loading directly (whereby a certain normal threshold load serves as a baseline for activity, and deviations from this baseline 'trigger' a cascade of cellular events) to those involving indirect stimuli induced by mechanical loading. Such stimuli include load-induced fluid flow, which provides the actual mechanism for mechanotransduction at a cellular level (e.g. *via* shear stresses). It has been postulated (Piekarski and Munro, 1977; Knothe Tate and Niederer, 1998) and proved *ex vivo* (Knothe Tate and Knothe, 2000) that load-induced fluid flow is a decisive contributing mechanism for the movement of interstitial fluid in the relatively impermeable tissue of compact bone. In addition to its hypothesized role in mechanotransduction, the displaced fluid serves as a carrier for the metabolites, nutrients, mineral precursors and osteotropic agents that are important for cellular activity.

If load-induced fluid flow enhances the transport of these key substances, then convective transport could play an additional role in regulating cellular activity associated with the processes of functional adaptation and remodelling. To address these issues, molecular tracer methods previously developed by our group (Knothe Tate et al., 1998b) were applied *in vivo* to study the effects of load-induced fluid displacements under controlled four-point bending loads. A semiquantitative analysis of tracer distribution was carried out to address two questions, namely (i) whether load-induced fluid flow enhances the transport of regulating agents, and (ii) whether tracer distribution could be related to specific areas within the cross section as well as to loading mode. Finally, these observations and analyses were interpreted in the light of the functional adaptation response to loading regimes, using the same *in vivo* model, to determine whether fluid flow can be correlated to the mechanically adaptive cellular response.

Materials and methods

In vivo experiments were conducted in 24 adult female, Sprague Dawley rats (240–320 g). All experiments were approved by an institutional animal care and oversight committee, and all procedures were carried out in compliance with the guiding principles set forth by the *American Journal of Physiology*. To ensure that the loading history remained well-defined, all rats were anaesthetised with pentobarbitone solution (Nembutal, 60 mg kg^{-1}) immediately before tracer injection and loading; they remained anaesthetised until killed. Through a lateral tail vein, 12 rats were injected with a 0.8 % Procion Red solution and 12 more rats with a bolus of microperoxidase dissolved in 0.9 % saline solution, prepared according to the methods of Knothe Tate et al. (1998b). The basic concept was to observe the influence of mechanical loading on short- and long-term molecular transport in rat bone. In general, the rate of transport for a given tracer decreases with increasing molecular mass and, for metabolically inactive tracer species, smaller molecules are transported more rapidly than larger ones. Thus, analogous to previous diffusion studies (Knothe Tate et al., 1998b), the low-molecular-mass (300–400 Da) Procion Red tracer was chosen to visualise short-term tracer transport (i.e. of the order of minutes) and the larger-molecular-mass (1800 Da) microperoxidase tracer to visualise long-term tracer transport (of the order of hours). Procion Red solution was injected immediately before loading, and microperoxidase was injected 2 h prior to loading.

Mechanical loads were applied using a four-point-bending device based on the model of Turner et al. (1991), whereby compressive loads were applied to the skin covering the soft tissues and bone of the lateral and medial surface, producing net bending that placed the medial tibia in tension and the lateral tibia in compression (Fig. 1). The left tibia served as an

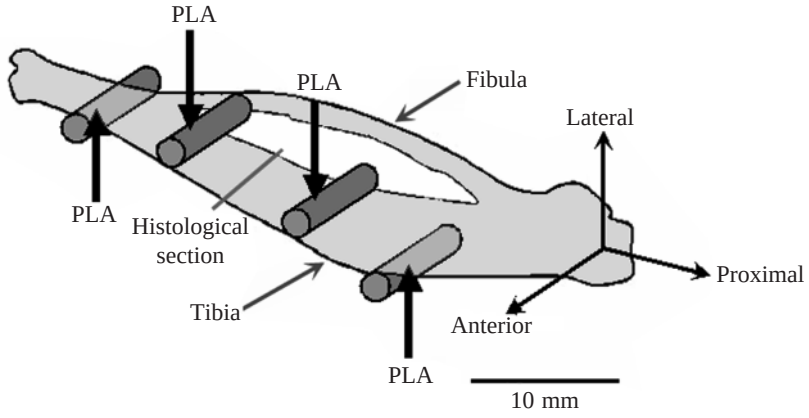

Fig. 1. A four-point-bending device is used to apply controlled mechanical loads to the right tibia of an anaesthetised rat. This schematic diagram depicts points of load application (PLAs) for four-point-bending *via* the cylindrical pads (upper pads 11 mm apart, lower pads 23 mm apart) as well as the position at which sections were taken for semiquantitative histological analysis. The fibula does not interfere with loading. In the case of the sham group, the two lower load application points directly apposed the two upper points with a span of 11 mm, causing a transverse compression load to be applied to the tibial shaft.

unloaded, contralateral control. Each group of 12 rats injected with either Procion Red or microperoxidase was subdivided further into four groups (of three rats each), each of which was subjected to 35 cycles of a 65 N amplitude load at three different frequencies (0.2, 2.0 and 5.0 Hz), analogous to previously published *in vivo* functional adaptation experiments using the same model (Turner et al., 1994). The fourth group was a 'sham' group, designed to control for the effects of trauma or periosteal pressure, in which a mainly compressive load was applied transverse to the axis of the right tibia.

After completion of loading, the rats were killed by exposure to CO_2. The left and right tibiae were then excised and processed according to the protocols of Knothe Tate et al. (1998b) for histomorphometric analysis. Undecalcified, polymethylmethacrylate-embedded specimens (50 μm) were prepared in the case of the Procion-Red-injected tibiae, and thin (approximately 6 μm) frozen sections were prepared from the tibiae injected with microperoxidase. Sections were taken from the middle of the bending area, 5.5 mm from the innermost loading pads (Fig. 1). A semiquantitative analysis of digitised micrographs from the sections of Procion-Red-injected rats was carried out to describe tracer distribution as a function of location within the cross section and as a function of mechanical loading variables, including primary loading mode and frequency. First, the sections were observed under a microscope (Leitz, Germany) using transmitted light (2.5× lens) for an overview of section geometry, and a selective green light excitation (Neofluor 10× lens, excitation maximum, 565 nm; emission maximum, 610 nm; mercury lamp and filter set) was then used to document tracer distribution. Transmitted light images were documented on Kodak Ektachrome 64T (tungsten) slide film, and fluorescent images were documented on Fujichrome Provia 400 slide film. All photographic slide images were scanned electronically, and the digital images were processed using Photoshop 4.0 software.

To begin the analysis, vascular spaces were removed from the fluorescent images using a colour- and edge-detection feature of Photoshop to prevent counting artefacts. Subsequently, the images were transformed to eight-bit grey-scale images, and a collage (piecing the individual images together to recreate the whole bone cross section) was produced to match the overview geometry as documented in transmitted light mode. Tracer distribution was related to loading mode by calculating a neutral axis for each bone cross section geometry and projecting the calculated neutral axis for each cross section onto the corresponding digitised image collage (Fig. 2). Eight 45° sectors (A1, A2, A3, M, L, P1, P2, P3) were defined using the neutral axis and the centroid as an origin (Fig. 2).

To count the number of osteocytes exhibiting tracer within a given area of each cross section (Fig. 2), NIH Image v. 3.56 was used to set thresholds and for particle counting. The number of fluorescing periosteocytic spaces was counted in each sector of all sections (blinded) and summed to determine the number of fluorescing spaces within areas corresponding to primary loading modes (compression and tension bands) for each loading frequency group (see Figs 2, 3). Because of natural colour variations in the microperoxidase staining, this semiquantitative method was not appropriate for the analysis of the presence and distribution of microperoxidase reaction product. Thus, sections from microperoxidase-injected rats were evaluated qualitatively under the light microscope (Leitz, Germany) to assess tracer distribution in comparison with the Procion-Red-injected rats.

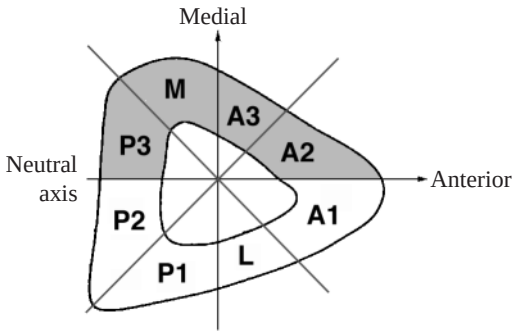

Fig. 2. The rat tibia in cross section. Regions where photomicrographs were taken are marked as M, A1–A3, L, P1–P3. The neutral axis, the centroid (the intersection between the neutral axis and a vertical line), the tension band (shaded) and the compression band (unshaded, below the neutral axis) are also depicted.

To relate tracer distribution to loading and to specific regions within the cross section of the loaded and unloaded tibia, a repeated-measures analysis of variance (ANOVA) was carried out (using StatView and Super Anova) for all the tibia pairs of the non-sham animals (N=9 pairs). To relate tracer distribution to mechanical loading variables, including loading frequency (i.e. 0.2 Hz, 2.0 Hz, 5.0 Hz) and primary loading mode (i.e. compression or tension) experienced by a given area of tissue, a repeated-measures ANOVA was applied to all tibia pairs, including those within the sham group (N=12 pairs). A significance level of $P<0.05$ was chosen for each analysis.

Results

Mechanical loading enhanced the transport of both the small- (Procion Red) and large- (microperoxidase) molecular-mass tracers within the bony tissue of the tibial mid-diaphysis. In addition, mechanical loading showed a highly significant effect on the number of periosteocytic spaces exhibiting tracer within the cross section of each bone. Pooling data from all loading groups (i.e. at frequencies 0.2 Hz, 2.0 Hz and 5.0 Hz) for each cross-sectional location, the concentration of Procion Red tracer was significantly higher in all areas within the cross sections of the tibiae subjected to pure bending loads than in those of the unloaded, contralateral tibia (N=9 pairs, $P<0.007$) (Fig. 3). Qualitative comparison of small- (i.e. Procion Red) and large- (i.e. microperoxidase) molecular-mass tracer transport showed faster transport of smaller molecular species through the tissue.

Furthermore, the enhancement of transport was significantly

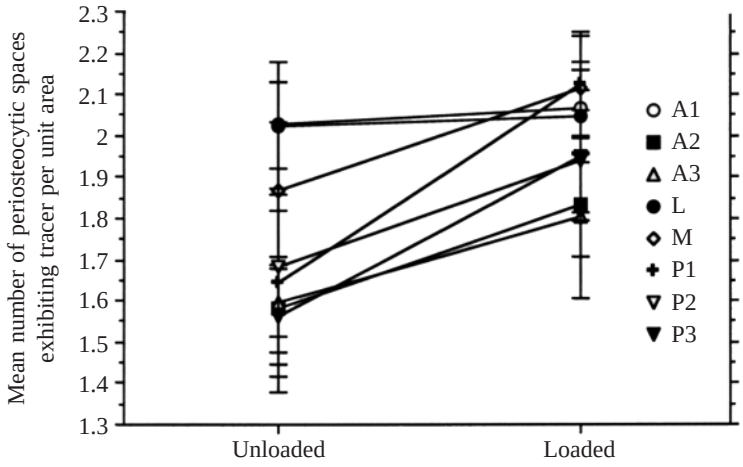

Fig. 3. Interaction plot showing the effects of loading on the distribution of Procion Red tracer (quantified as the mean number of periosteocytic spaces exhibiting tracer per unit area, μm^2) within the cross section of the mid-diaphysis. For each location A1, A2,..., P3 (for reference, see Fig. 3), mean values are derived from nine tibia pairs. Values are means ± S.E.M.

site-specific (N=9 pairs, P<0.04). For example, in the anterolateral corner of the cross section (i.e. the area corresponding to A1 in Fig. 2), minimal differences in tracer distribution were observable in the photomicrographs from the unloaded and loaded sides (Fig. 4A,B). In contrast, differences in tracer concentration and distribution were evident in photomicrographs taken from the area corresponding to P3 (Fig. 4C,D). The semiquantitative analysis, in which the number of periosteocytic spaces exhibiting Procion Red tracer was counted and normalised for area, corroborated these qualitative observations (Fig. 5).

In the three groups of tibiae subjected to pure bending loads and injected with Procion Red tracer, it could be shown that tracer distribution was highly dependent on loading effects (i.e. unloaded *versus* loaded). Within individual groups, differences attributable to primary loading mode (i.e. tension or compression band, Fig. 6) were significant in the 0.2 Hz, 2.0 Hz and sham-loading groups. Pooling data from all groups loaded in pure bending and unloaded controls, significant differences in the number of periosteocytic spaces exhibiting tracer could be shown between the unloaded and loaded sides of the tissue within the tension (P<0.003) and compression (P<0.04) bands of tissue ('tension' and 'compression bands' do not exist in the unloaded tibia cross section, but are defined analogously to those areas of the loaded tibia cross section). Although a significant difference could be shown between the tissue corresponding to tension and compression bands of the unloaded tibiae (P<0.04), no significant difference was observed between the two different loading modes in the loaded tibiae.

Regardless of loading mode, the mean difference in the number of periosteocytic spaces exhibiting tracer between the loaded right side and the unloaded contralateral side decreased with increasing loading frequency (Fig. 7). There was a significant difference between the 2.0 Hz and 5.0 Hz loading groups (N=6 pairs, P<0.04) as well as between the 5.0 Hz and sham-loading groups; the difference between the 0.2 Hz and 2.0 Hz loading group was not significant. In the sham-loading group, the area corresponding to the tension band of the groups exposed to pure bending loads was actually subjected to transverse compressive loads. Within this area, a reduction in tracer concentration was observed in comparison with the unloaded contralateral side. In contrast, the area corresponding to the compression band of the groups exposed to pure bending exhibited similar results to those of the other groups, indicating that transverse compressive loading resulted in an increased tracer concentration in comparison with the unloaded contralateral side.

Discussion

It has been suggested that extravascular fluid flow through bony tissue occurs as a natural effect of mechanical loading in poroelastic bone tissue. Shear stresses produced by the drag of this flow on the surfaces of osteocytes and their processes have been postulated to serve a role in mechanotransduction. Furthermore, in moving through the lacunocanalicular system, this fluid carries metabolites, nutrients, mineral precursors and osteotropic agents important for cellular activity. We hypothesise that, by enhancing the transport of such key substances, fluid flow driven by mechanical deformation serves an additional role in regulating cellular activity associated with the processes of functional adaptation and remodelling. To test this hypothesis, we applied tracer methods previously developed by our group (Knothe Tate et al., 1998b) to observe load-induced fluid displacements *in vivo* under controlled four-point-bending loads. Our results indicate that mechanical loading promotes molecular transport significantly within the relatively impermeable matrix of cortical bone. Furthermore, tracer distribution varies among regions within the cross section as well as with mechanical loading variables including loading mode and loading frequency. The mean difference (loaded side–unloaded side) in the number of periosteocytic spaces exhibiting the Procion Red tracer is significantly higher within the areas corresponding to the tension band than in those within the compression band of the cross section for the groups loaded at frequencies below 5.0 Hz, although differences in tracer distribution between loaded and unloaded tibiae decrease as loading frequency increases.

The interrelationships between tracer concentration and

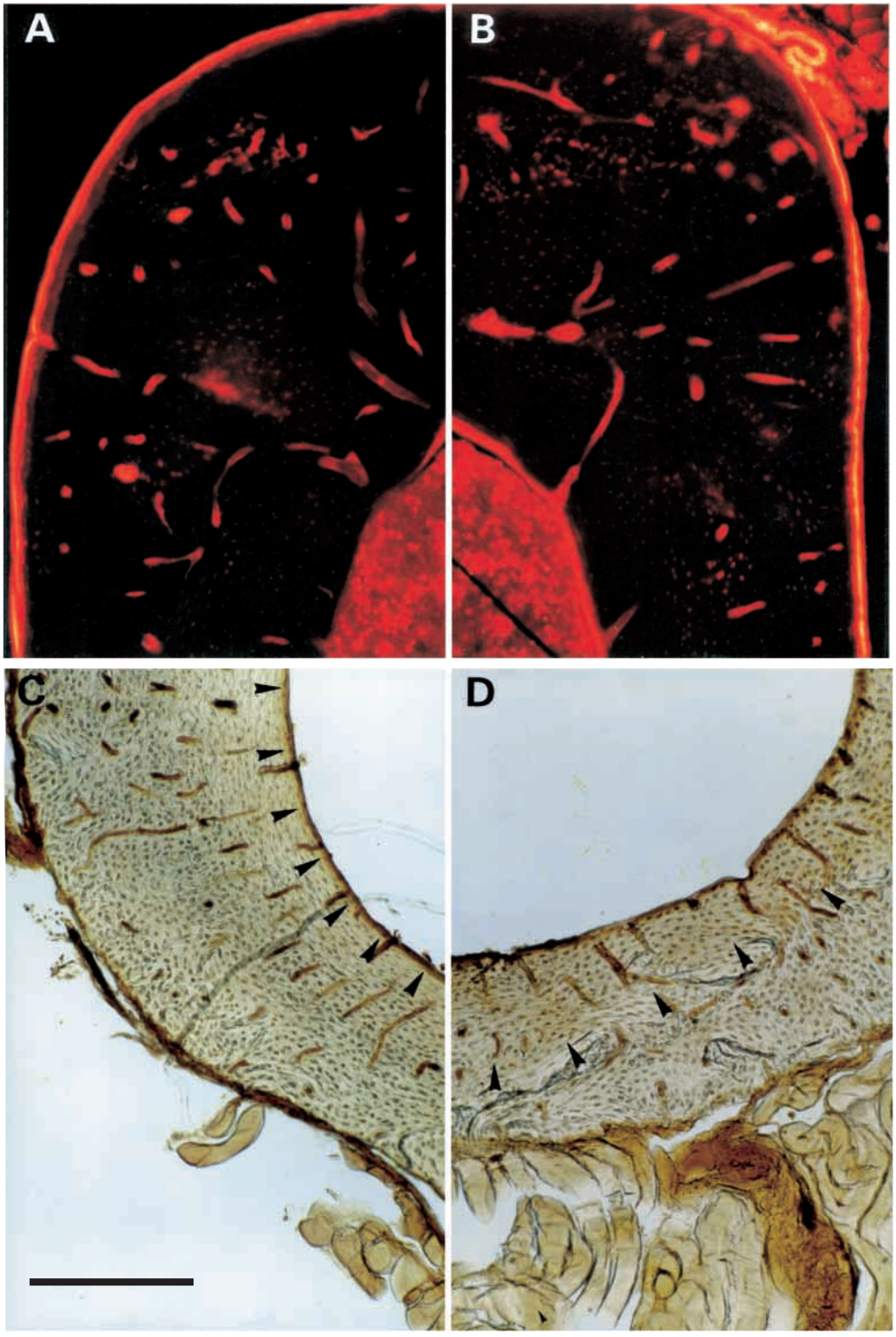

Fig. 4. (A,B) Procion Red tracer photomicrographs from the aspect of the tibial cross section corresponding to A1 in Fig. 2 taken with the 40× objective. The distribution of tracer in the loaded (36 cycles at 0.2 Hz) specimen (B) is similar to that in the unloaded contralateral control (A). (C,D) Microperoxidase tracer photomicrographs from the aspect of the tibial cross section corresponding to P3 in Fig. 2. The difference in depth of penetration of the rust-brown-coloured tracer in the loaded (36 cycles at 0.2 Hz) tibia (D) and the unloaded contralateral control (C) is apparent (the arrowheads demarcate the line of tracer penetration). Scale bar, 1 mm.

loading mode and between loading mode and loading frequency may provide the first experimental evidence that load-induced fluid flow occurs *in vivo*. It has been shown in previous studies (Knothe Tate et al., 1998b) that both the tracers used are transported extravascularly and extracellularly *via* the lacunocanalicular system; thus, fluid displacements visualised by differential tracer concentrations between the loaded and unloaded bones are indicative of transport induced by fluid flow and not by active (e.g. intracellular) transport mechanisms. Our results indicate that fluid displacements induced by mechanical loading affect the transport of solutes contained within the interstitial fluid in bone tissue, moving smaller molecular species (e.g. Procion Red) faster than larger ones (e.g. microperoxidase). The observed enhancement of molecular transport in response to mechanical loading corroborates earlier *in vitro* and *ex vivo* experimental data

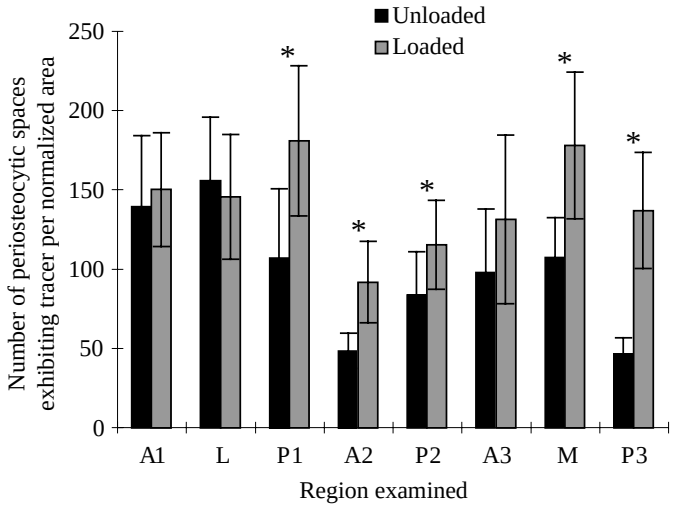

Fig. 5. Mean number of periosteocytic spaces exhibiting Procion Red tracer (N=12 pairs) under loaded and unloaded conditions, normalized for area. Values are means ± S.E.M. Regions showing significant differences between the loaded and unloaded sides are marked with an asterisk (P1, A2, P2, M and P3).

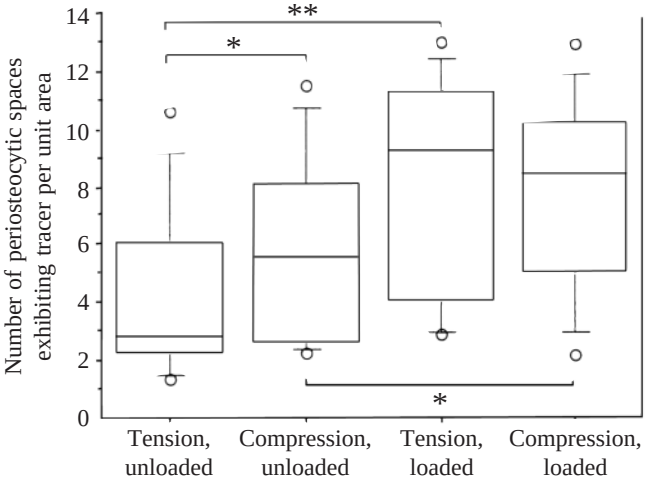

Fig. 6. Box plot showing the number of periosteocytic spaces exhibiting tracer per unit area (μm^2) for each loading mode of the unloaded and loaded tibiae from all groups, excluding the sham group. Asterisks represent significant differences between treatments (*P<0.04, **P<0.003). The horizontal line within the box represents the median, the vertical lines are the upper and lower fences, and the circles are outlying data points.

(Knothe Tate et al., 1997, 1998a,b; Knothe Tate and Knothe, 2000).

Strain-related differences in tracer distribution provide support for the hypothesis that modelling and remodelling in bone tissue is regulated in part by the differential transport of osteotropic substances through the tissue (Knothe Tate and Niederer, 1998). Although it is not possible to measure strain and tracer distribution in the same experiment because preparation of the bone surface to accommodate strain gauges would alter fluid displacements, the fluid flow data reported in

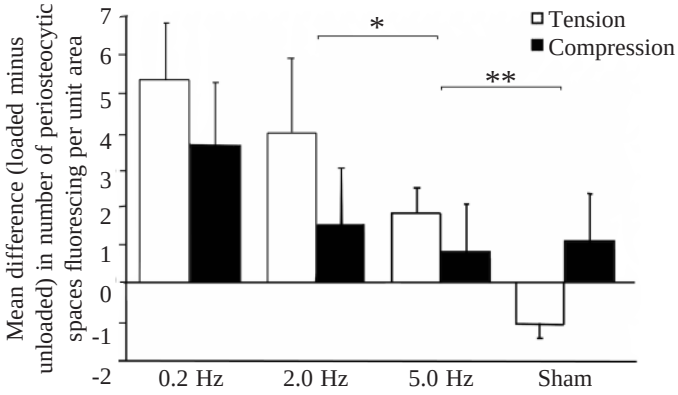

Fig. 7. Interaction bar chart showing the difference (loaded minus unloaded, standard error bars) in number of periosteocytic spaces exhibiting Procion Red tracer throughout whole tibia sections (N=12 pairs) for each loading mode and frequency, expressed per unit area (μm^2). Asterisks represent significance levels between treatments (*P<0.04, **P<0.01).

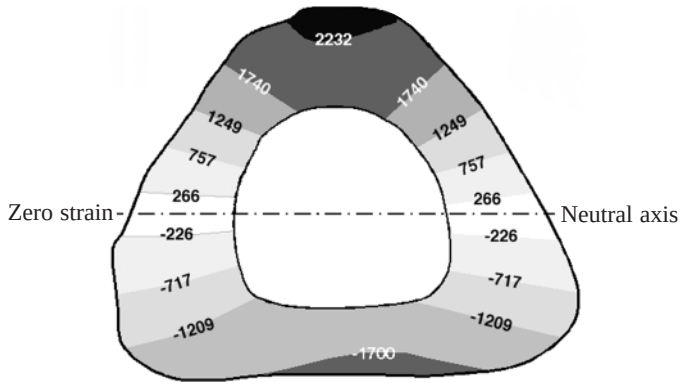

Fig. 8. Strain distribution within the cross section at the middle of the bending lever as predicted by finite-element analysis (after Akhter et al., 1992). A four-point-bending load (35 N) is applied such that the medial surface is in tension (maximum strain 0.2232 % or 2232 microstrain) and the lateral surface (maximum strain –0.17 % or –1700 microstrain) is in compression. In this study, a 65 N load was applied, engendering a maximum load of 0.291 % (2910 microstrain) on the periosteal surface, with strain decreasing down to zero at the neutral axis.

this study can be related to the strain magnitudes and distributions of the four-point-loading system described by Akhter et al. (1992) and Forwood et al. (1998). In the present study, 65 N loads were applied *via* the loading pads; on the basis of strain measurements of rat tibiae, a linear relationship between applied load and strain has been demonstrated. Hence, for the loads applied in this study, peak strains of approximately 2910 microstrain (or 0.291 % strain) would result at the periosteal surface, decreasing to zero strain at the neutral axis.

On the basis of a finite-element analysis of the tibial cross section (Akhter et al., 1992), the medial aspect of the cross section is subjected to higher strains than the lateral aspect (Fig. 8). This results from the asymmetry of the bone (cross-

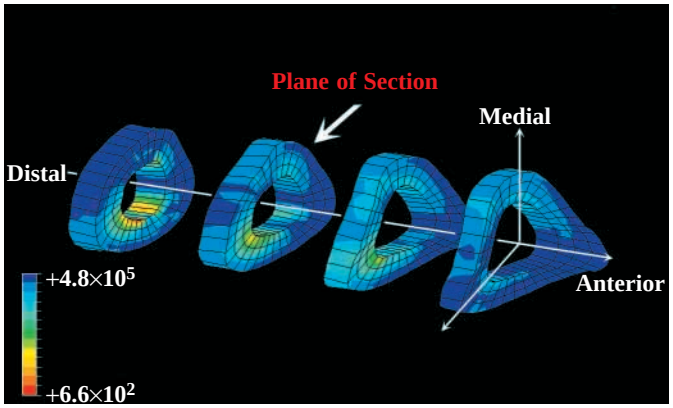

Fig. 9. Fluid velocity magnitudes along the length of the rat tibia, with the tibiofibular junction (distal end) on the left side. Velocities are represented as nondimensional colour scale values (after Steck et al., 1999).

sectional asymmetry), from bone curvature (which has an effect on the moment of inertia) and from the greater distance from the medial surface to the centroid of the section (producing a greater moment arm). Thus, one would expect fluid displacements through the medial aspect to be larger than those through the lateral aspect. This may explain why the area corresponding to the tension band of the cross section (the portion medial to the neutral axis) exhibits a higher tracer concentration than the area corresponding to the compression band (the portion lateral to the neutral axis). Another possibility is that tracer distribution reflects loading mode *per se*; e.g. if the spaces through which the fluid flows exhibited directional differences in resistance to flow or if the Poisson's ratio of the tissue caused displacements in one plane to be larger in tension and those in the orthogonal plane to be larger in compression such that one loading mode promoted movement of fluid preferentially in the longitudinal direction and the other promoted flow in the radial direction. These effects would not be expected to be as pronounced at high loading frequencies, at which the viscoelastic properties of the tissue become prominent. Although we were not able to elucidate these relationships in this study, by incorporating serial as well as longitudinal sections in future study designs, these effects might be understood.

Differences in tracer distribution due to differences in strain distribution or loading modes within the tissue can be distinguished from site-specific differences due, for example, to proximity to the blood supply, because reported data relating to strain distribution always depict the difference between the loaded and unloaded sides, thus reflecting load-induced displacements and subtracting out local microanatomical effects.

The strain-related differences in tracer distribution observed in this study have been corroborated by data from *in vitro* and *ex vivo* experimental studies and computer modelling studies (Knothe Tate and Knothe, 2000; Knothe Tate et al., 1997, 1998a; Steck et al., 1998), in which it has been shown that strain distribution affects fluid flow and hence tracer distribution. Poroelastic computer models of the rat tibia

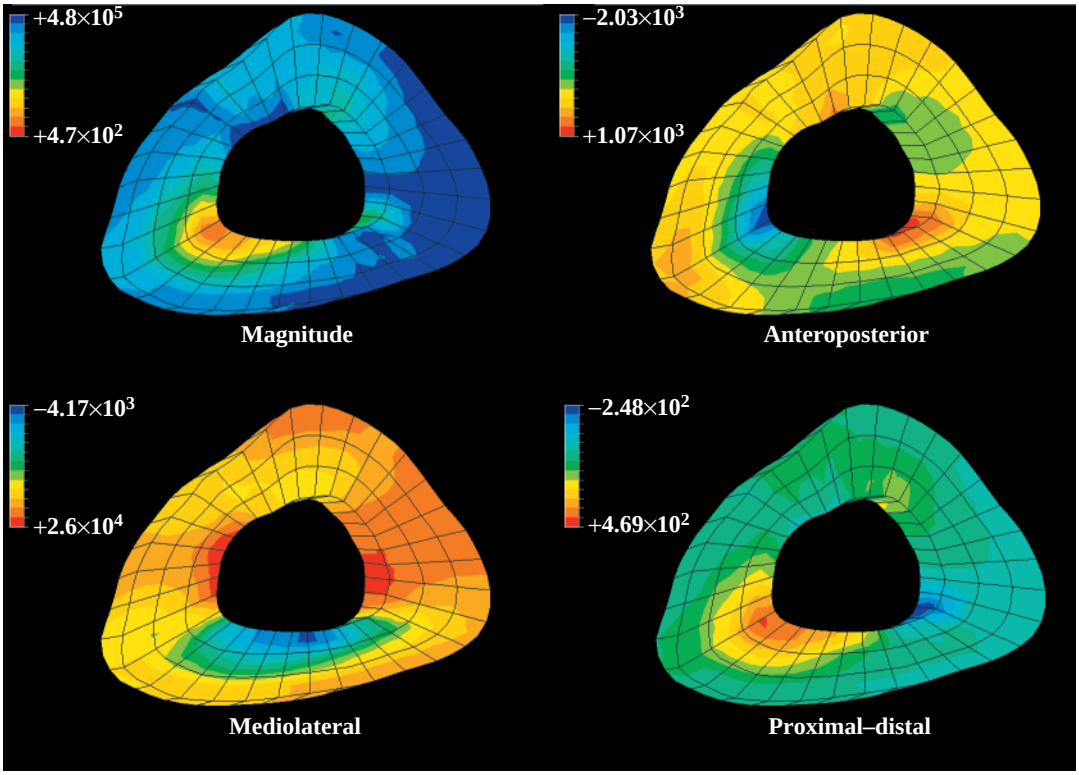

Fig. 10. Fluid velocity magnitude and three scalar components (clockwise from top right) in the anteroposterior, proximal–distal and mediolateral directions. The calculations were made on the section indicated by the white arrow in Fig. 9. Velocities are represented as nondimensional colour scale values (after Steck et al., 1999).

currently in development (Steck et al., 1999) allow strain distributions and fluid displacements throughout the tissue to be predicted, aiding significantly in correlating strain and tracer distributions. Whereas the strain distribution curve of the tibia in cross section (Fig. 8) reflects the strain state in that plane at maximal loading magnitude, corresponding plots of velocity magnitude distribution in the tibia underscore the complex nature of the three-dimensional problem (Fig. 9). In fact, on the basis of highly idealised isotropic models of the rat tibia, it appears that the mediolateral component of the velocity vector in the plane of the section (reflecting the direction of bending) best approximates the distribution of tracer in the histological specimen. For example, the area corresponding to P3 (Fig. 2) shows a very high fluid velocity in the mediolateral direction (Fig. 10). The areas corresponding to P1 and L show a low fluid velocity along the endocortex in the mediolateral direction and a somewhat larger fluid velocity periosteally; averaging the two within the area representing P1 or L results in a lower than average velocity. This supports the idea that the high fluid velocities occurring in the direction of bending have the largest effect on the distribution of tracer.

The effect of loading frequency on tracer distribution is interesting, because it has been hypothesized that smaller-magnitude loads, applied at higher frequencies, might provide as potent a stimulus, for example for the maintenance of bone mass, as loads of higher magnitude at lower frequencies (Rubin and McLeod, 1994). Furthermore, it has been suggested that strain rate may be an important controlling variable in the functional adaptation response to altered mechanical loading conditions (Mosley and Lanyon, 1998). Although we observed a general trend in which differences in the presence of tracer between the loaded and unloaded side decreased with increasing loading frequency, this observation may reflect simple differences in the duration of exposure to the tracer. However, as mentioned above, the decrease in the difference between the loaded and unloaded sides may reflect the viscoelastic behaviour of bone loaded at higher frequencies, at which the tissue 'stiffens' as result of a lack of time for the fluid pressure to relax between loading cycles. Loading frequency and rate effects are being elucidated in experiments designed specifically to calculate diffusion coefficients and tracer distribution under a variety of loading frequencies, rates and durations *in vitro* (Knothe Tate et al., 1997).

Interestingly, new bone that forms as an adaptive response to the four-point-bending loads (observed in another set of experiments carried out under analogous conditions, with the same loading model) (Turner et al., 1994) develops in areas corresponding approximately to those experiencing the lowest fluid velocities in the mediolateral direction (the direction of bending). As described previously (Turner et al., 1994), at loads greater than 40 N (a threshold), lamellar bone formation is stimulated at the endocortical surface, away from the loading at the periosteal surface. This lamellar bone formation at the endocortical surface is regarded as being indicative of an adaptive response to the application of a bending load. At the periosteal surface, a woven bone response is elicited, which is not considered to be a truly adaptive response. Rather, the woven bone formation observed on the periosteal surfaces reflects the effects of bending and periosteal pressure and thus represents either an inflammatory or a traumatic response. Turner et al. (1994) reported endocortical bone formation rates to be greatest at the medial and lateral surfaces and least at the surfaces along the neutral axis (anterior and posterior surfaces). This is consistent with an association between regions of greatest bone formation rates and lowest fluid velocities occurring in the direction of bending along the endocortical surface (Fig. 10). Thus, although the medial and lateral cortices are exposed to high strains, the mediolateral component of the fluid velocity vector (i.e. in the direction of bending) is lowest along the endocortical surface of the medial and lateral cortices of the mid-diaphyseal cross section.

To our knowledge, this is the first experimental validation in which a relationship between load-induced fluid flow and functional adaptation could be demonstrated experimentally. Our experimental and theoretical data suggest that mechanical loading, e.g. *via* four-point-bending of the tibia, modulates local flow distribution and concentration profiles within the tissue. Furthermore, on the basis of *in vitro* and *ex vivo* experimental data (Knothe Tate and Knothe, 2000; Knothe Tate et al., 1997), local architecture and hydraulics also appear to modulate interstitial flow distribution and mass transport at the cellular level, which would be expected to affect cell viability and signalling. Further studies using markers of cell viability and activity, together with fluid flow tracers, should be carried out to test these possibilities.

Somewhat conflicting results were obtained for the sham group, in which the rat tibiae were subjected primarily to transverse compressive loads. Surprisingly, differences between the loaded and unloaded sides were observed in these tibiae, raising the question of the extent to which the experimental model represents a non-invasive situation *per se*. Such differences, particularly the suppression of fluid transport in response to loading of the medial aspect of the tibia (the area corresponding to the tension band of the animals exposed to four-point bending) may be an indicator of pressure-induced ischaemia during loading, of fluid displacements caused by transverse loading or of both. Although it might be argued that the effects of periosteal pressure may be negligible as long as one limits the observation of the adaptive response to endosteal areas of bone (since these areas would be unaffected by any periosteal effects), this may not be a valid assumption in the light of our fluid flow data. On the basis of the data from this and other studies (Knothe Tate and Knothe, 2000), we expect that the whole cross section will be affected by such effects, i.e. as soon as perfusion and/or differential transport of fluid is affected by loading, these effects can no longer be regarded as local phenomena (and thus cannot be neglected in local areas). Furthermore, if the extravascular fluid flow across the cross section is affected by local loading effects, then the osteotropic agents carried by this fluid will also be affected, thus altering the adaptive cellular response throughout the cross section. More study of these influences seems warranted.

Given the promising association between theoretical predictions of fluid flow induced by four-point-bending regimes, the actual concentration and distribution of bone fluid tracers *in vivo* and the remodelling response in analogous experimental models, it is likely that load-induced fluid flow plays a regulatory role in processes associated with functional adaptation. Further studies testing the correlation between load-induced fluid flow and specific cellular activities are required to evaluate the exact role of fluid flow in such processes.

The authors gratefully acknowledge Iris Keller for her assistance with histological and histochemical processing of the specimens. This project was supported in part by a grant from the Swiss National Science Foundation (3200-049796.96/1) and a National Health and Medical Research Council (Aust) Project Grant (961245).

References

Akhter, M. P., Raab, D. M., Turner, C. H. and Recker, R. R. (1992). Characterization of *in vivo* strain in the rat tibia during external application of a four-point bending load. *J. Biomech.* **25**, 1241–1246.

Chambers, T. J., Evans, M., Gardner, T. N., Turner Smith, A. and Chow, J. W. M. (1993). Induction of bone formation in rat tail vertebrae by mechanical loading. *J. Bone Miner. Res.* **20**, 167–178.

Cowin, S. C., Moss-Salentijn, L. and Moss, M. L. (1991). Candidates for the mechanosensory system in bone. *J. Biomech. Eng*. **113**, 191–197.

Dawson, T. M. and Snyder, S. H. (1994). Gases as biological messengers: nitric oxide and carbon monoxide in the brain. *J. Neurosci.* **14**, 5147–5159.

Forwood, M. R., Bennett, M. B., Blowers, A. R. and Nadorfi, R. L. (1998). Modification of the *in vivo* four-point loading model for studying mechanically induced bone adaptation. *Bone* **23**, 307–310.

Fox, S. W., Chambers, T. J. and Chow, J. W. M. (1995). Nitric oxide as an early mediator of the induction of bone formation by mechanical strain. *J. Bone Miner. Res.* **10**, S204.

Frangos, J. A., Eskin, S. G., MacIntyre, L. V. and Ives, C. L. (1985). Flow effects on prostacyclin production by cultured human endothelial cells. *Science* **227**, 1477–1479.

Hillam, R. A. and Skerry, T. M. (1995). Inhibition of bone resorption and stimulation of formation by mechanical loading of the modeling rat ulna *in vivo*. *J. Bone Miner. Res.* **10**, 683–689.

Klein-Nulend, J., van der Plas, A., Semeins, C. M., Ajubi, N. E., Frangos, J. A., Nijweide, P. J. and Burger, E. H. (1995). Sensitivity of osteocytes to biomechanical stress *in vitro*. *FASEB J.* **9**, 441–445.

Knothe Tate, M. L. and Knothe, U. (2000). An *ex vivo* model to study transport processes and fluid flow in loaded bone. *J. Biomech.* **33**, 247–254.

Knothe Tate, M. L., Knothe, U. and Niederer, P. (1998a). Experimental elucidation of mechanical load-induced fluid flow and its role in bone metabolism and functional adaptation. *Am. J. Med. Sci.* **316**, 189–195.

Knothe Tate, M. L. and Niederer, P. (1998). A theoretical FE-based model developed to predict the relative contribution of convective and diffusive transport mechanisms for the maintenance of local equilibria within cortical bone. In *Advances in Heat and Mass Transfer in Biotechnology* (ed. S. Clegg), pp. 133–142. New York: The American Society of Mechanical Engineers.

Knothe Tate, M. L., Niederer, P. and Knothe, U. (1998b). *In vivo* tracer transport through the lacunocanalicular system of rat bone in an environment devoid of mechanical loading. *Bone* **22**, 107–117.

Knothe Tate, M. L., Niederer, P., Tepic, S. and Perren, S. M. (1997). *In vitro* investigation of deformation-induced fluid displacement in small cylindrical specimens excised from cortical sheep bone (abstract). *Trans. Orthop. Res. Soc.* **43**, 801.

Mason, D. J., Hillam, R. A. and Skerry, T. M. (1996). Constitutive *in vivo* mRNA expression by osteocytes of β-actin, osteocalcin, connexin-43, IGF-I, c-*fos* and c-*jun*, but not TNF-α nor tartrate-resistant acid phosphatase. *J. Bone Miner. Res.* **11**, 350–357.

Mosley, J. R. and Lanyon, L. E. (1998). Strain rate as a controlling influence on adaptive remodeling in response to dynamic loading of the ulna in growing male rats. *Bone* **23**, 313–318.

Pead, M. J., Suswillo, R., Skerry, T. M., Vedi, S. and Lanyon, L. E. (1988). Increased ^{3}H-uridine levels in osteocytes following a single short period of dynamic loading *in vivo*. *Calcif. Tissue Int.* **43**, 92–96.

Piekarski, K. and Munro, M. (1977). Transport mechanism operating between blood supply and osteocytes in long bones. *Nature* **269**, 81–82.

Pitsillides, A. A., Rawlinson, S. C. F., Suswillo, R. F. L., Bourrin, S., Zaman, G. and Lanyon, L. E. (1995). Mechanical strain-induced NO production by bone cells: a possible role in adaptive bone (re)modeling? *FASEB J.* **9**, 1614–1622.

Rawlinson, S. C. F., Pitsillides, A. A. and Lanyon, L. E. (1996). Involvement of different ion channels in osteoblasts' and osteocytes' early responses to mechanical strain. *Bone* **19**, 609–614.

Rubin, C. and Lanyon, L. (1984). Regulation of bone formation by applied dynamic loads. *J. Bone Jt. Surg.* **66**A, 397–402.

Rubin, C. and McLeod, K. J. (1994). Promotion of bony ingrowth by frequency-specific, low-amplitude mechanical strain. *Clin. Orthop.* **298**, 165–174.

Steck, R., Knothe Tate, M. L., Niederer, P. and Schneider, E. (1998). Theoretical modelling of load-induced fluid displacement in compact bone. In *Poromechanics* (ed. J. F. Thimus, Y. Abousleiman, A.-H. D. Cheng, O. Coussy and E. Detournay), pp. 511–516. Rotterdam: A. A. Balkema.

Steck, R., Niederer, P. and Knothe Tate, M. L. (2000). Prediction of load-induced fluid flow in bone and its implications for transport phenomena, *Computer Methods in Biomechanics and Biomedical Engineering* (ed. J. Middleton). Amsterdam: Gordon & Breach Publishers.

Torrance, A. G., Mosley, J. R., Suswillo, R. F. L. and Lanyon, L. E. (1994). Noninvasive loading of the rat ulna *in vivo* induces a strain-related modeling response uncomplicated by trauma or periosteal pressure. *Calcif. Tissue Int.* **54**, 241–247.

Turner, C. H., Akhter, M. P., Raab, D. M., Kimmel, D. B. and Recker, R. R. (1991). A noninvasive *in vivo* model for studying strain adaptive bone remodeling. *Bone* **12**, 73–79.

Turner, C. H., Forwood, M. R., Rho, J.-Y. and Yoshikawa, T. (1994). Mechanical loading thresholds for lamellar and woven bone formation. *J. Bone Miner. Res.* **9**, 87–97.

Turner, C. H., Owan, I., Takano, Y., Madalli, S. and Murrell, G. A. C. (1995). Nitric oxide plays a role in bone mechano-transduction. *J. Bone Miner. Res.* **10**, S235.